Activity and activity cycles of PLATO target stars: PIC implications

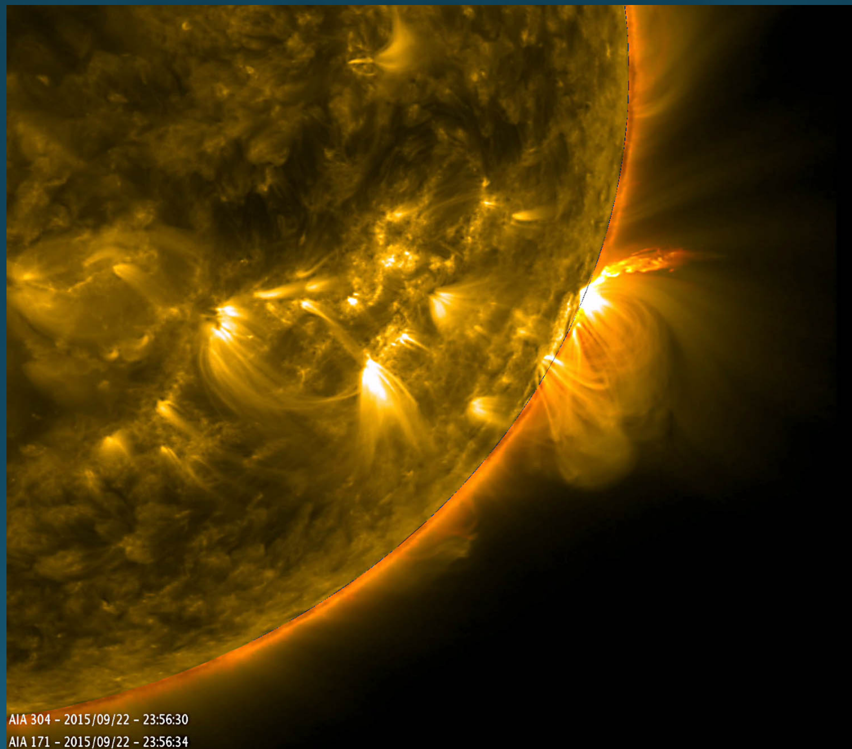

Image Credit: NASA/SDO

Antonino Francesco Lanza

INAF - Catania Astrophysical Observatory, Italy - PSM WP 123 000: Stellar rotation and activity

Stellar magnetic activity

- Stellar magnetic activity is the ensemble of *phenomena produced by magnetic fields in stellar atmospheres*;
- They are characterized by
  - spatial inhomogeneity;
  - time variability;
  - non-radiative heating;
  - modification of convection and turbulence spectra;
  - additional wave modes.

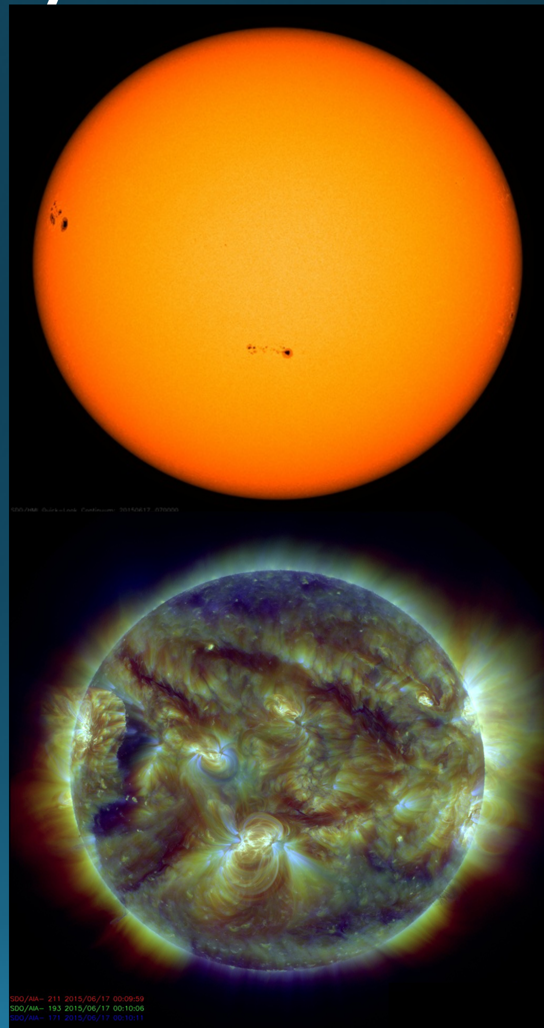

Why activity matters

- Activity affects the *detection of planets* and the *measurements of their parameters*, notably their mass (RV jitter) and radius (systematic modifications of the transit depths);

- An indication of the star activity level is required for confirming planetary candidates and determine the priority for their follow-up observations;

- Moreover, activity affects planets orbiting late-type stars through:
    - atmospheric evaporation (through EUV and X-ray fluxes);
    - the impact of high-energy radiation on habitability;
    - modulation of cosmic-ray flux by the interplanetary field.

Temperature in the solar atmosphere

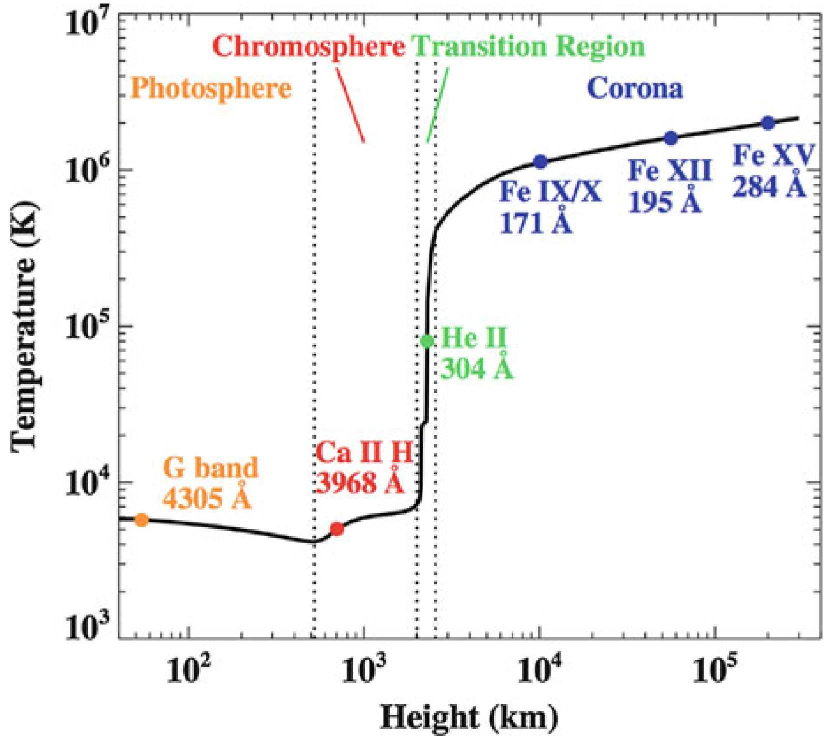

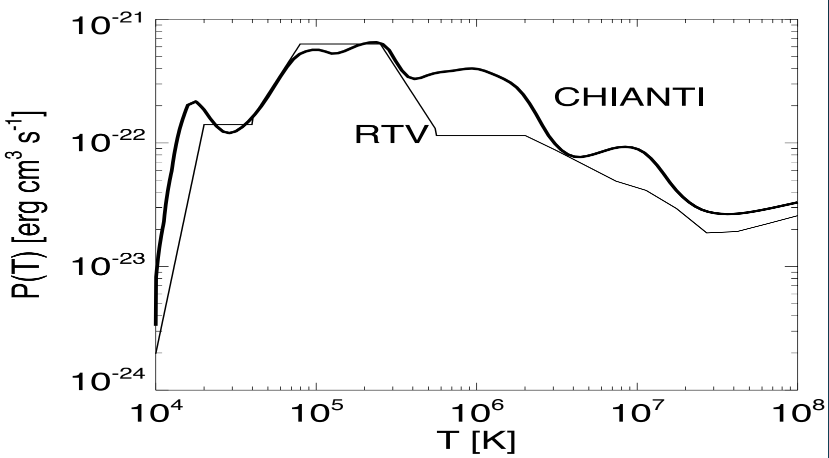

(Reale & Landi 2012)

(after Vidotto 2017; credits Yang et al. 2009)

Connection between different domains

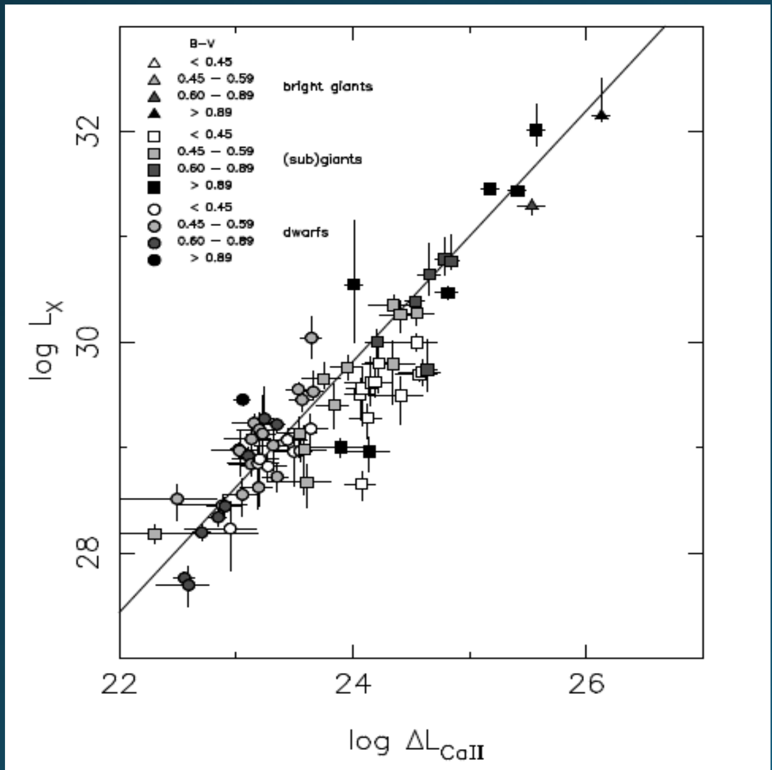

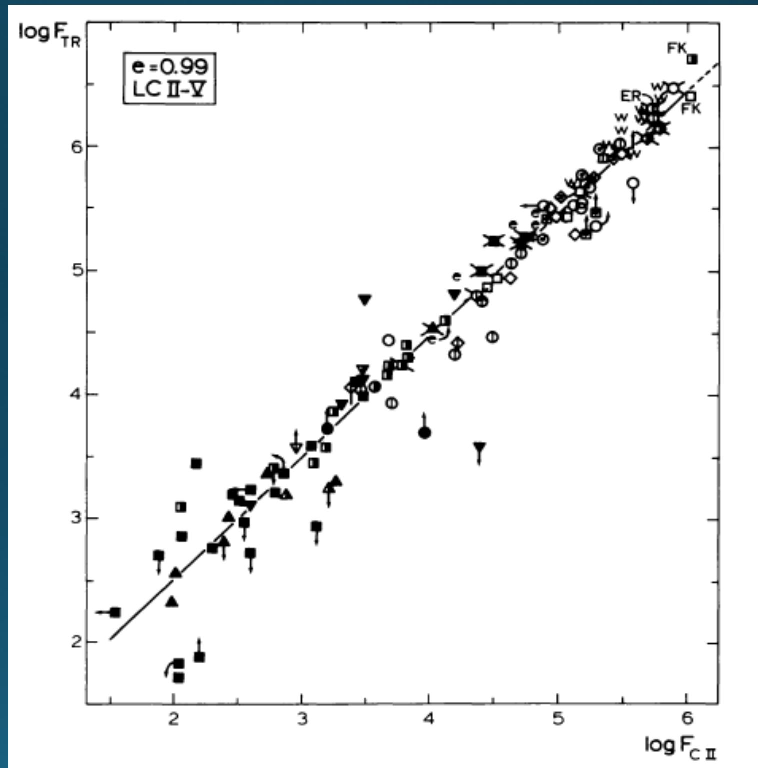

F_{TR} includes the flux in lines of NV, Si IV and C IV formed in the transition zone;

C II is the flux in the line at 133.5 nm; the various symbols define ranges in B-V and luminosity class of the stars.

Given the role of heat conduction from the corona and the magnetic origin of the heating, fluxes in chromospheric and transition regions lines are statistically correlated with each other and with the coronal X-ray flux. I show some examples above (Piters et al. 1997 on the left; Oranje 1986 on the right). See also Pagano (2013).

X-ray luminosity vs. Rossby number

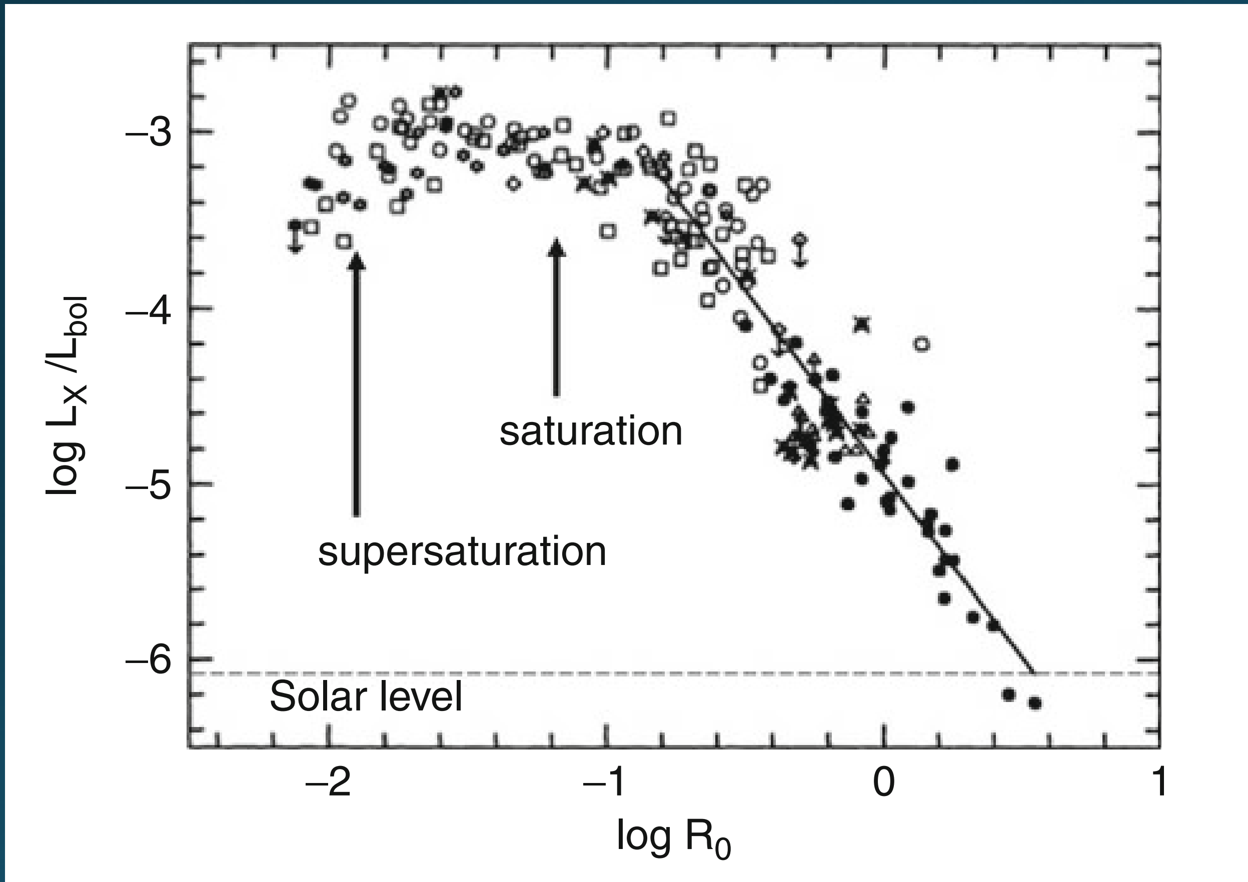

$R_O = P_{rot}/\tau_c$ (Rossby number)

(after Randich 2000; Pizzolato et al. 2003; Pagano 2013)

Stellar activity cycles

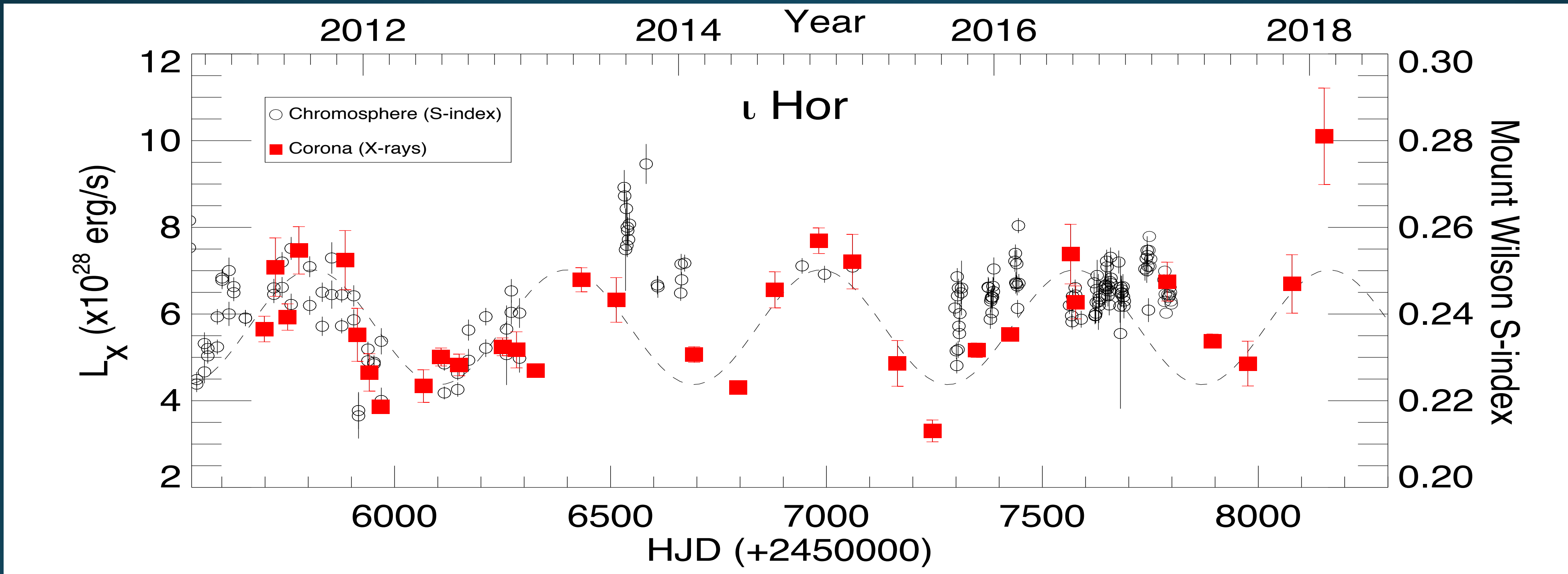

Iota Horologii (F8V/G0V, 600 Myr, log R'_{HK} =- 4.6) after Sanz-Forcada et al. (2019)

HD 81809 and the Sun

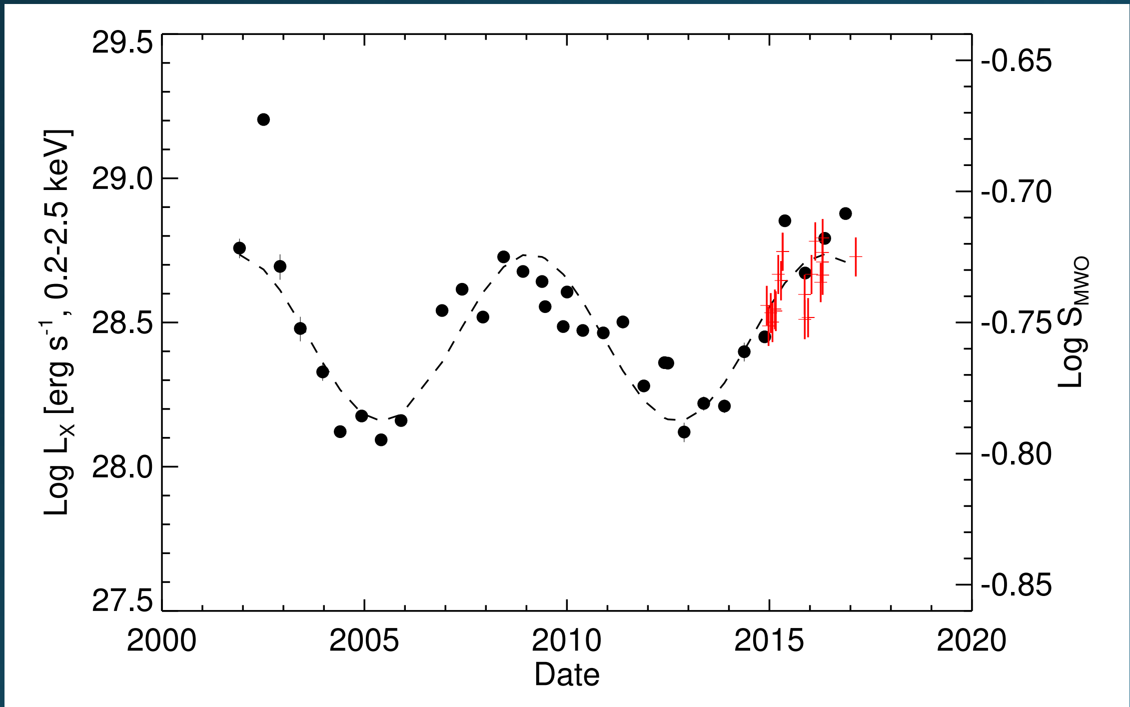

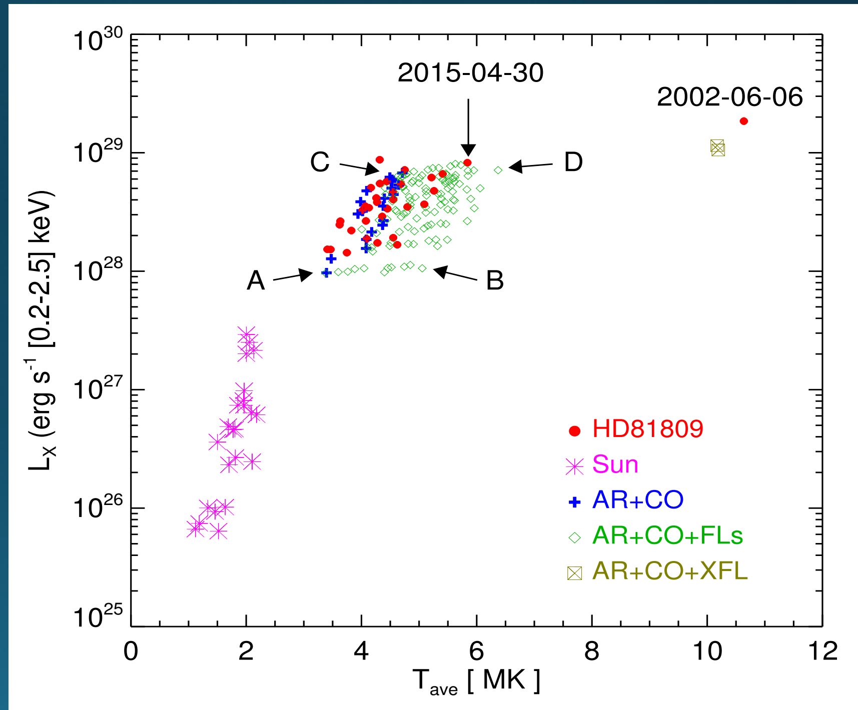

Coronal cycle of HD 81809 (a G-type star) and its modelling with different coronal components (Orlando et al. 2017).

The activity level decreases in time

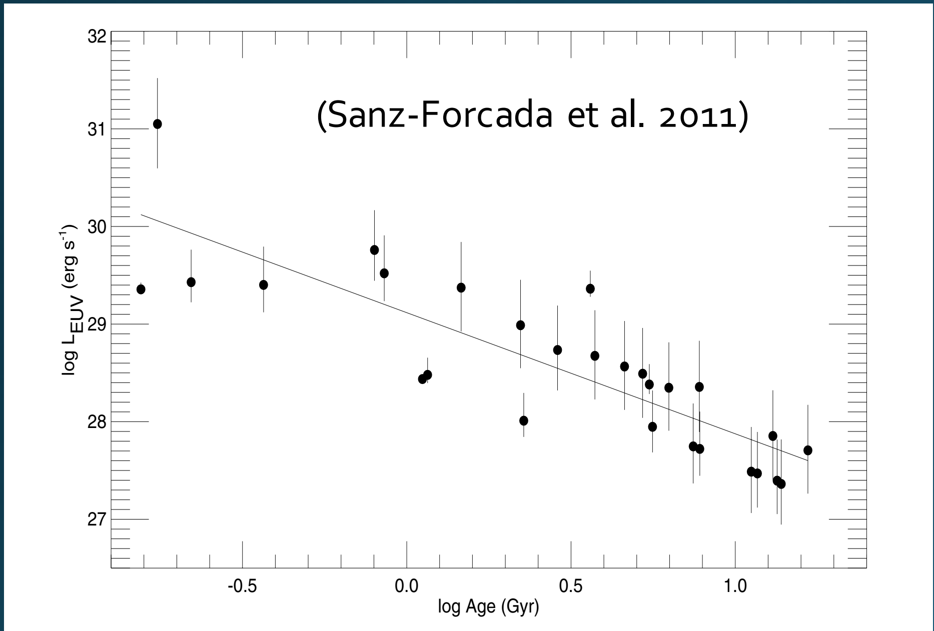

Fig. 3. Distribution of EUV luminosities against age (in Gyr) determined using the X-ray luminosities. The line indicates the best linear fit to the sample.

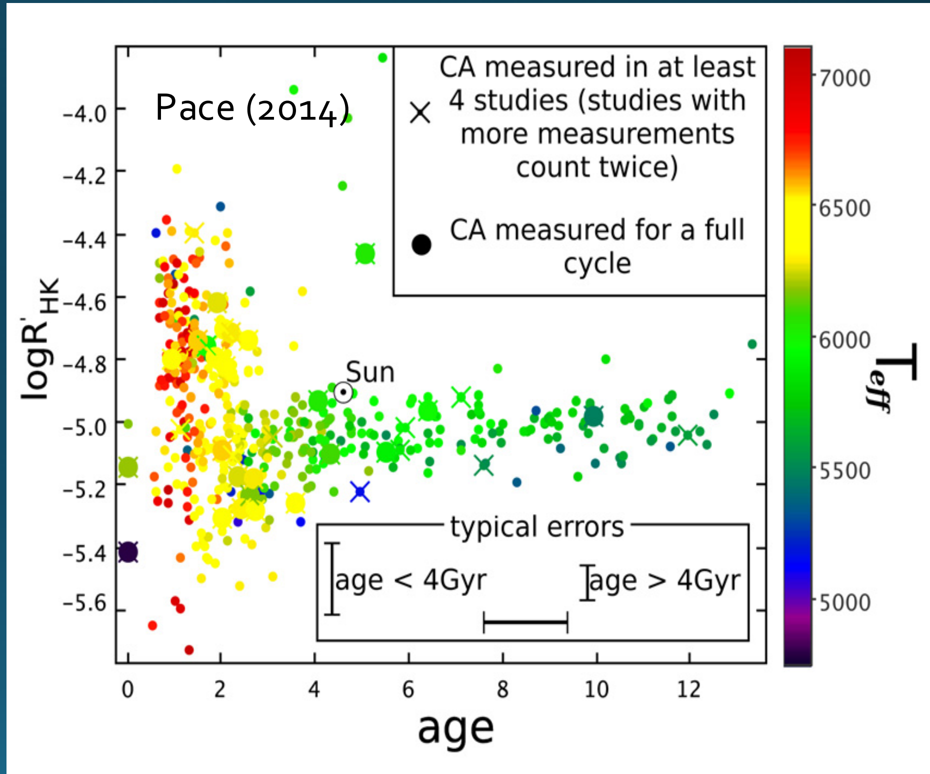

EUV passband: 10-92 nm

Log R'_{HK} measures the flux in the cores of the Ca II H&K lines

Stellar activity and planetary transits

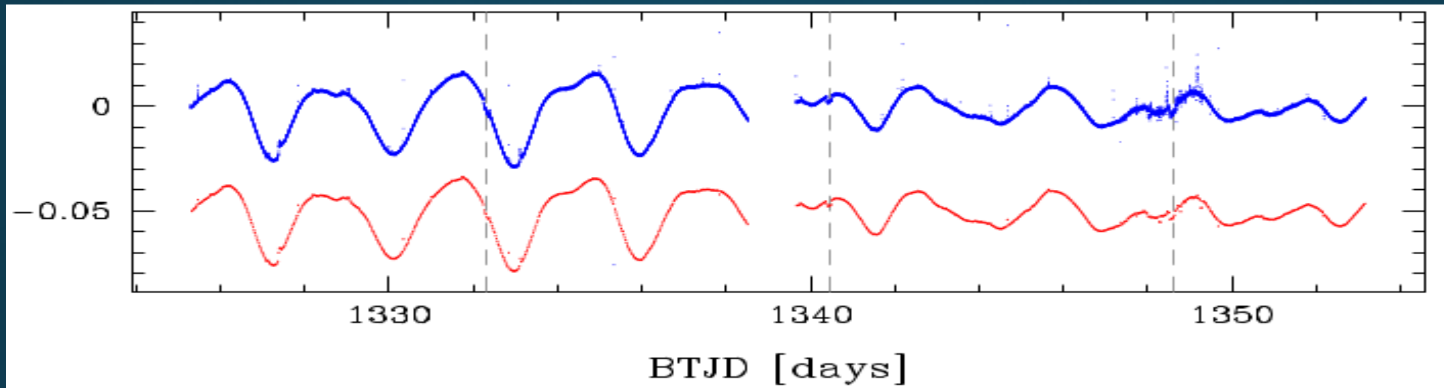

DS Tuc (TESS photometry)

(Benatti et al. 2019)

- Magnetic activity is not a serious limitation to detect transits of Earth-like planets in the case of middle-aged Sun-like stars (e.g., Aigrain & Irwin 2004; Moutou et al. 2005; Bonomo et al. 2009);
- measurements of the phase curves of giant planets or brown dwarfs (or ellipsoidal modulation or Doppler beaming) generally requires to model and remove activity effects;
- transit depths are affected by starspots, requiring a proper modelling to derive R_p/R_* (e.g., Ballerini et al. 2012).

Activity and Radial Velocity (RV) of the Sun as a star

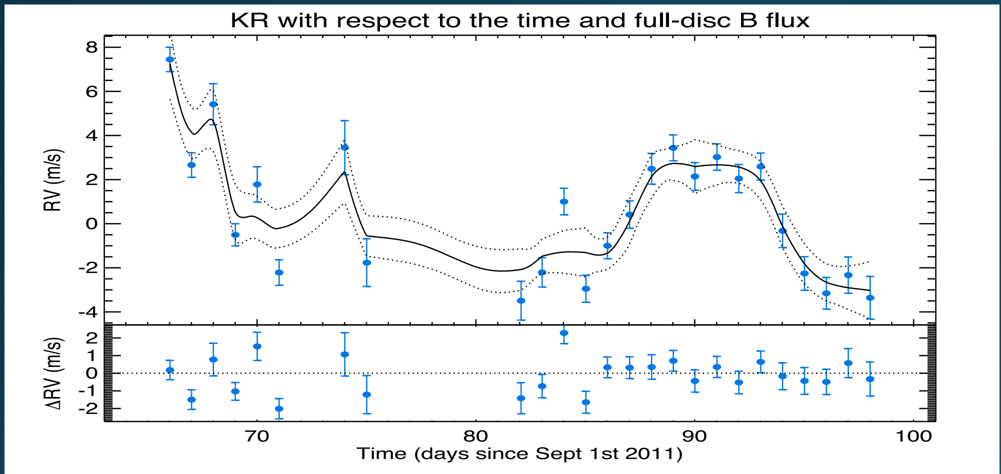

(Lanza et al. 2019; Haywood et al. 2016)

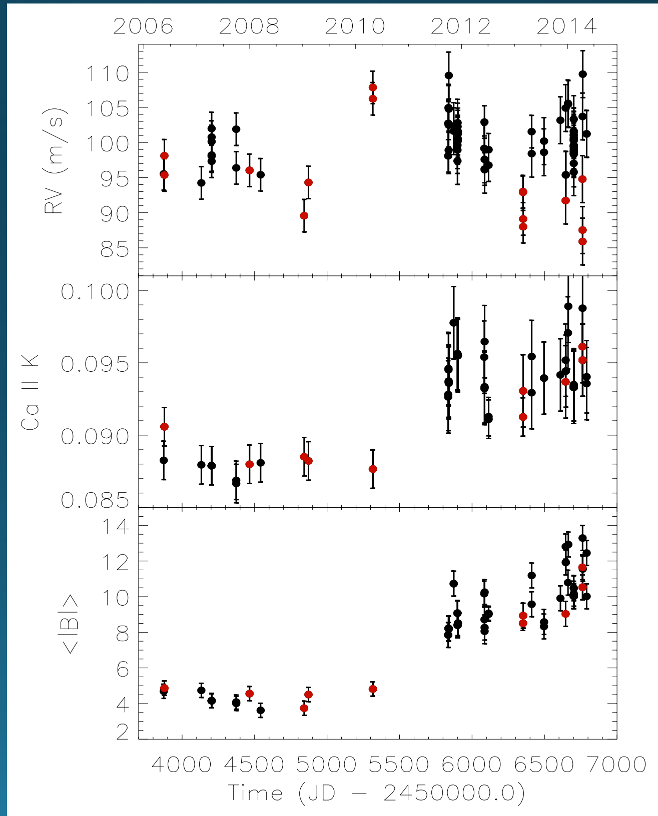

(Lanza et al. 2016)

Activity and Radial Velocity (RV) of the Sun as a star

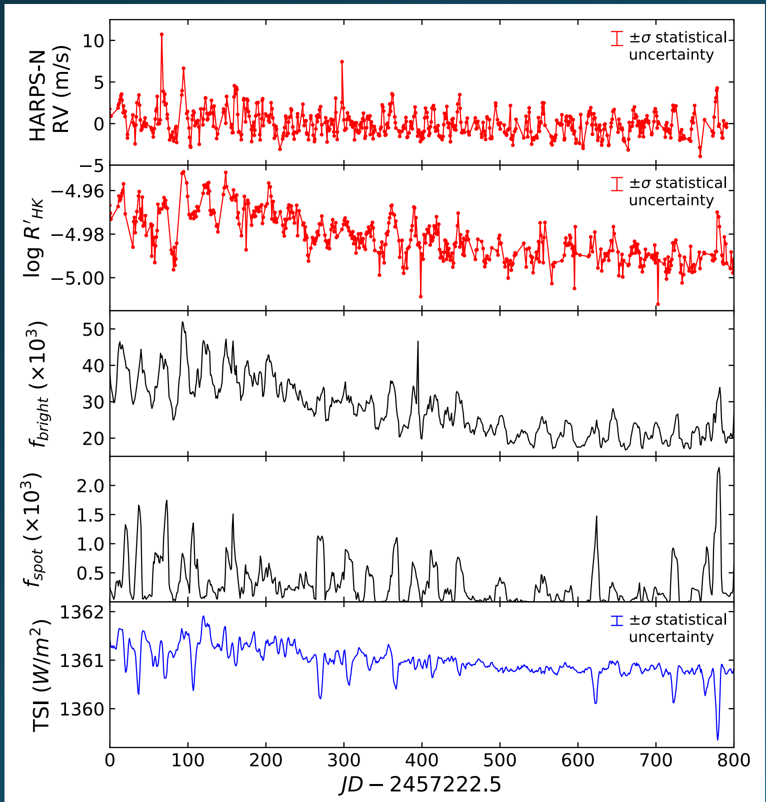

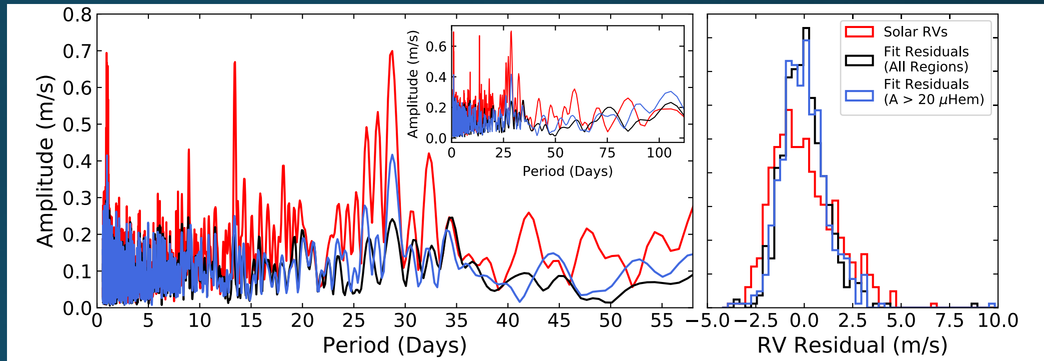

(Milbourne et al. 2019)

Activity and p-mode oscillations

- Activity produces a shift of the frequencies of p-mode in solar-like stars (e.g., Karoff et al. 2018; Garcia & Ballot 2019);
- The effect depends on the intensity and spatial distribution of the magnetic fields providing a way to measure activity cycles and differential rotation (e.g., Thomas et al. 2019);
- Activity tends to reduce the amplitude of p-modes which can be a problem for their detection is the case of young stars (Chaplin et al. 2011).
- This can affect measurements of stellar age, rotation, and inclination;
- Comparison of rotation measurements from astroseimology and rotational modulation of the flux are possible (e.g., Nielsen et al. 2015).

HD 173701 ($M=1.0M_\odot$, $R=0.93R_\odot$) Sun

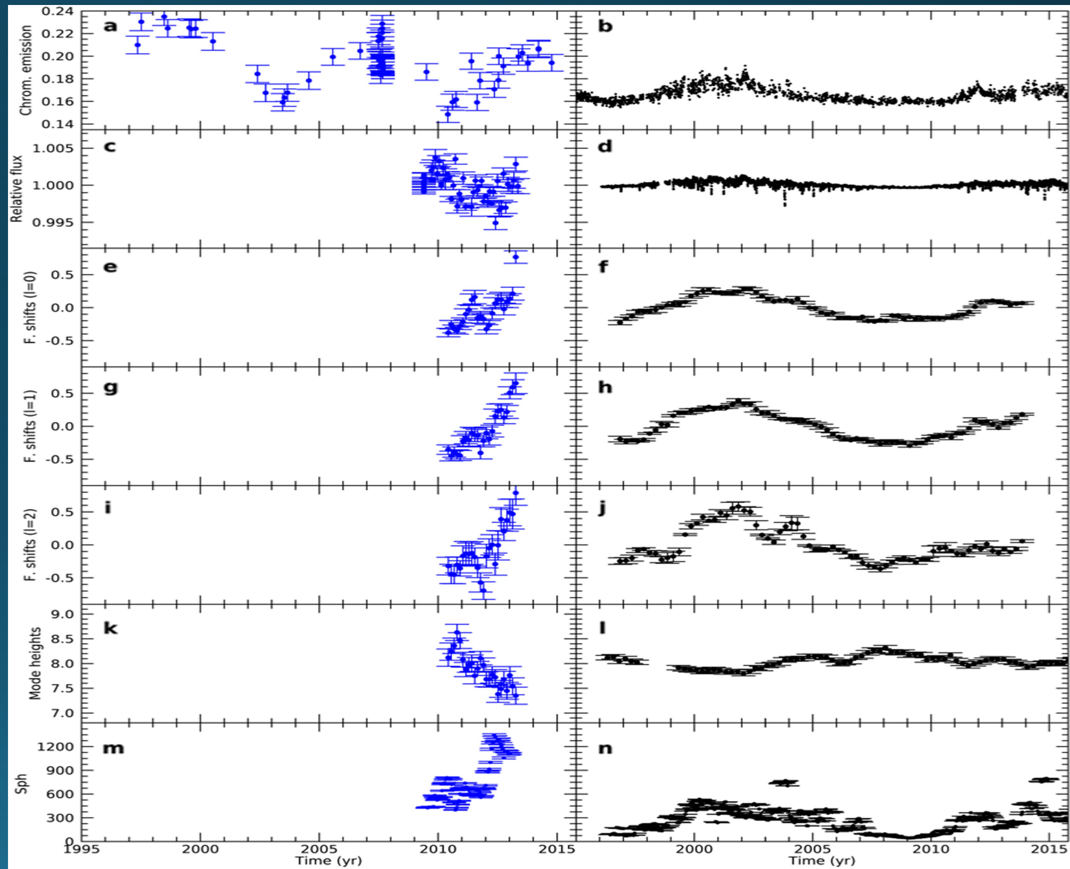

(HD173701: T_{eff} = 5490 K; P_{rot} = 21 d; P_{cycle} = 7.4 yr; Karoff et al 2018)

Solar irradiance along cycle 24 (SORCE)

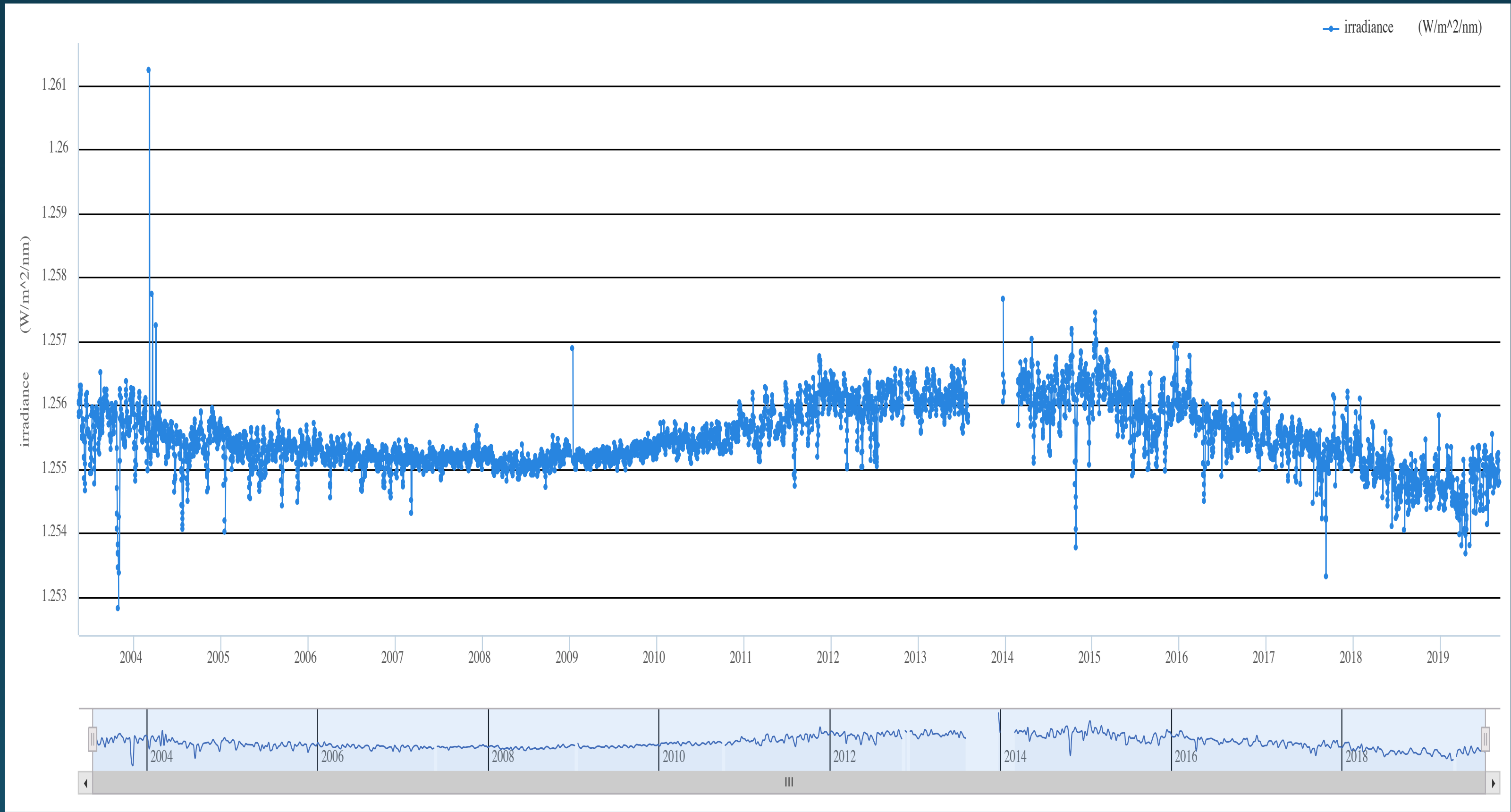

Long-term variation (LTV): $\Delta F/F \simeq 1.6 \times 10^{-3}$ at 748 nm; rotational modulation is between 10% and 150% of LTV; the Sun is brighter when more active (it's an ***activity-bright*** star [Radick et al. 2018; Shapiro et al. 2014; Meunier & Lagrange 2019]).

How to include activity information in PIC: some general considerations

- In a given passband, the amplitude of variability depends on the timescale;
- From the point of view of transit detection, a useful metrics could be similar to Kepler Combined Differential Photometric Precision (CDPP; Gilliland et al. 2015), that is, the overall noise on timescales of 3-12 hr;
- Given the statistic correlation between the flux in different passbands, data from X-rays and UV surveys can be used to characterize the activity level of stars;
- The amplitude of the cycle (and flare) variations increases with decreasing wavelength giving a larger dispersion in the EUV and X-rays at a fixed level of activity.

Possible activity proxies

- Amplitude of the optical variability (specify the passband and the timescale);
- Normalized X-ray (L_X / L_{bol}) or UV luminosities;
- Chromospheric indexes, notably Ca II H&K, Hα, or Ca IR triplet (requires high-res spectroscopy; for example: Gaia; Gaia-ESO; RAVE; GALAH; but consider limitations related to the survey purposes).

Example 1: Gaia photometry

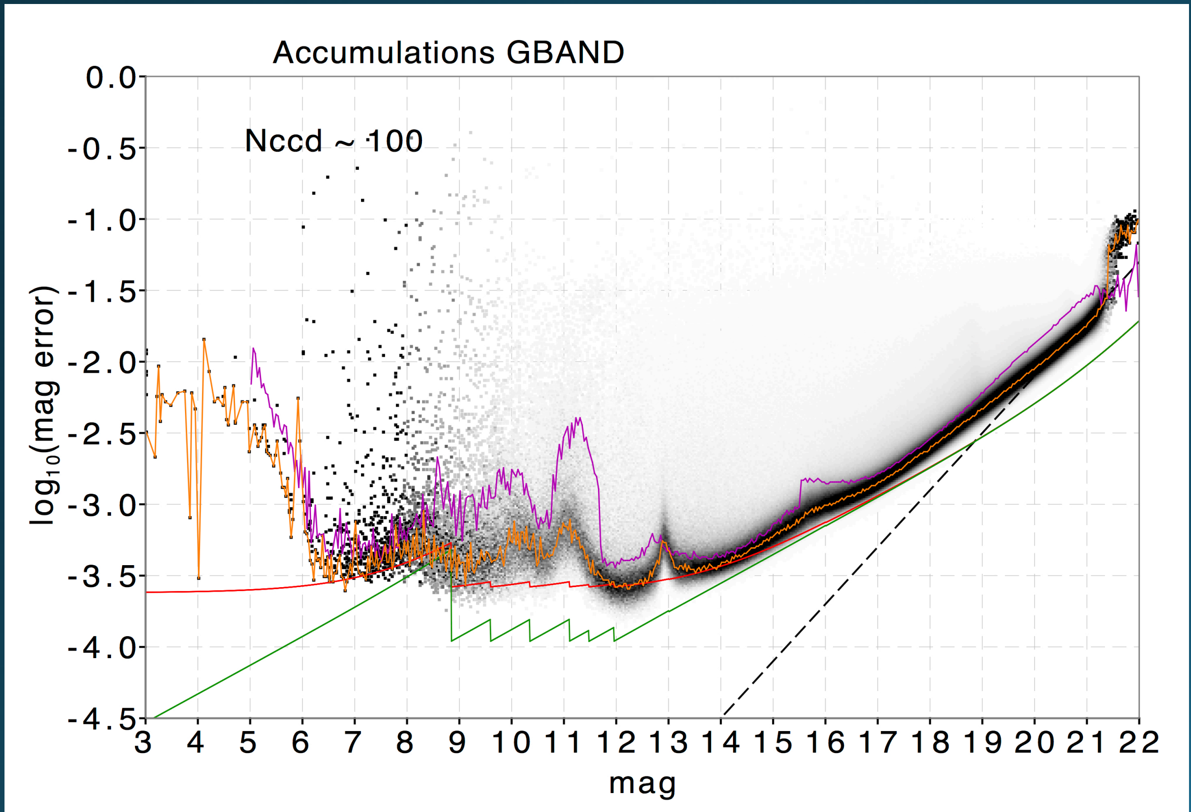

The main limitation of Gaia photometry from our point of view is the *scanning law*;

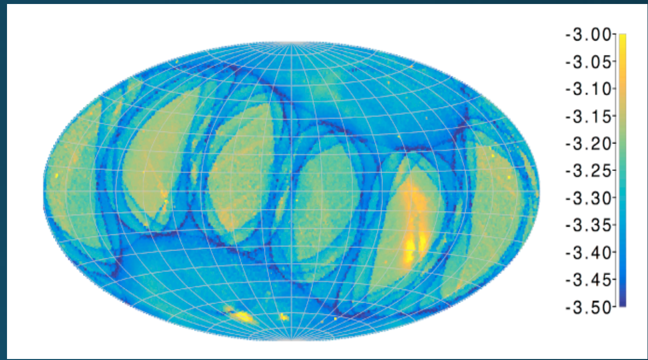

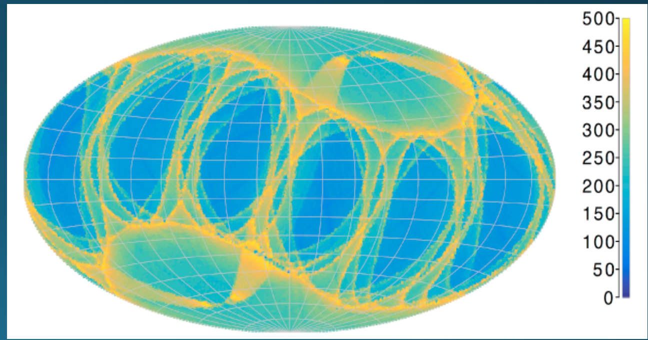

Left panel - *Orange line*: mode of the distribution in DR2; *magenta:* same in DR1; *green:* nominally expected with a perfect calibration; *red*: with calibration uncertainty of 2 mmag; the *dashed black line* with a slope of 0.4 shows that the faint end is sky-dominated (Evans et al. 2018).

Example 2: eRASS (eROSITA All Sky Survey):

eROSITA is a German instrument on the Russian SRG mission

- Next Generation all-sky X-ray survey
  - 30× deeper than ROSAT, 10× deeper than XMM-Slew
- All-Sky Surveys starting early 2020, 8 full surveys separated by 6 months

scanning: 4h / rotation → each sky position seen 6 x per day in each eRASS

All potential PLATO targets will be observed in eRASS.

Example: M dwarfs in d < 10pc

** 40% undetected to date*

** > 2 dex spread of X-rays for given SpT*

→ Understanding evolution of planet atmosphere requires to know XUV emission of every single host star

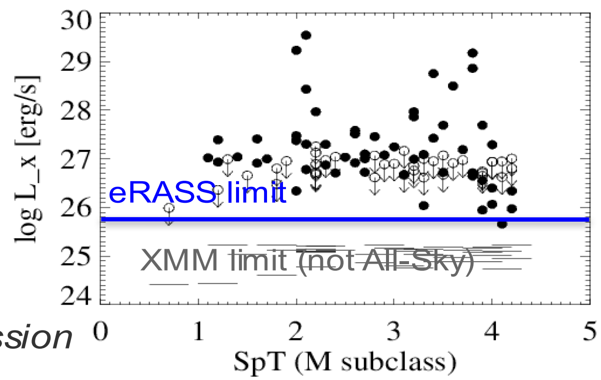

Expected number of stars in eRASS:

≈500 000 detections
(vs. ROSAT: ~ 60 000 new X-ray sources)

50 000 @ > 200 cts
→ X-ray temperature

5 000 @ > 1000 cts
→ detailed spectra

Conclusions

- PLATO targets should not be selected by discriminating against active stars because that will penalize young targets and lead to an excess of stars viewed with low inclination, if based on optical/IR variability;

- A measurement of the optical variability can be a useful proxy, although the variability on transit timescales can be derived in a systematic way only from some surveys (e.g., TESS, in part, Gaia);

- Surveys in the X-rays (ROSAT, eROSITA) and UV (GALEX) can be very useful, but one should keep in mind the flux variability produced by activity cycles, rotational modulation, and transients (flares); there is a bias towards younger, more active stars (except for targets closer than 10-25 pc);

- Rotational periods for large samples of stars in clusters and in the field (e.g., K2, Gaia) can be used together with activity-rotation relatioships to estimate the activity level.

Thank you for your attention

Additional material

Example 2: eROSITA

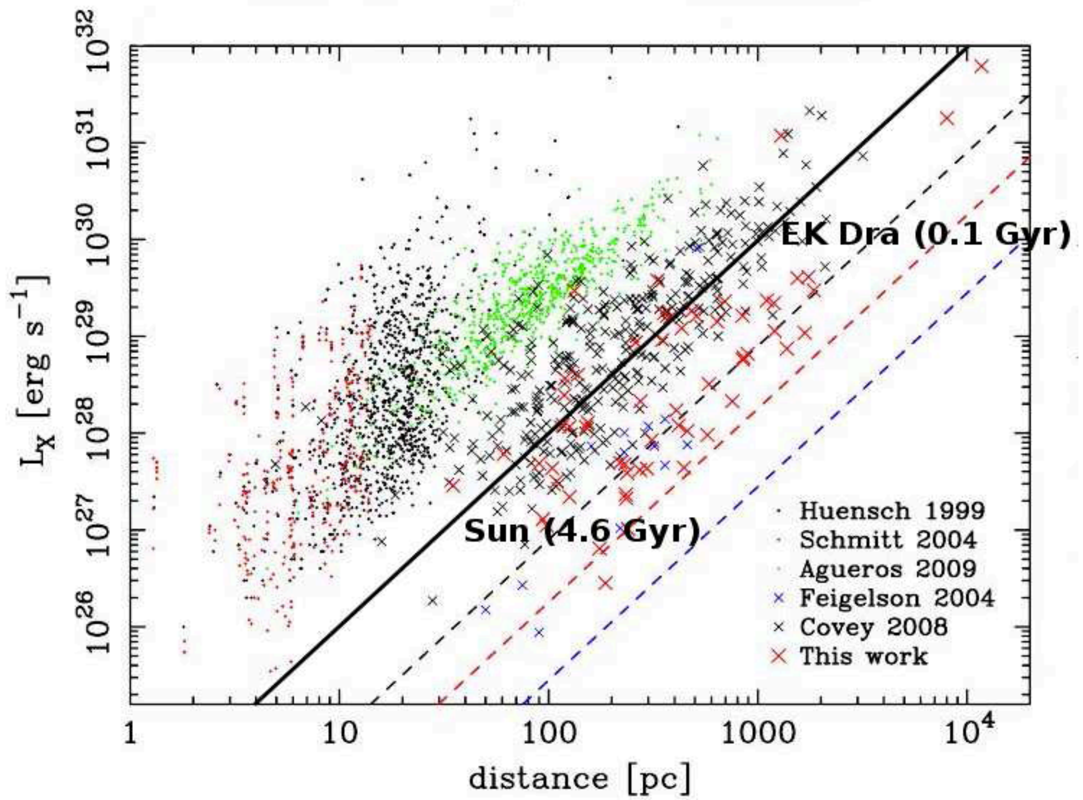

Figure 5.4.2: eROSITA all-sky survey sensitivity with two Suns (adapted from Wright et al. 2010). eROSITA sensitivity (black line) vs. stellar sources detected by ROSAT: survey + pointings (dots) and in Chandra deep imaging surveys: CDF-N, ChaMP and COSMOS (crosses).

(Merloni et al. eROSITA Science Book)

The Sun in the optical and in EUV

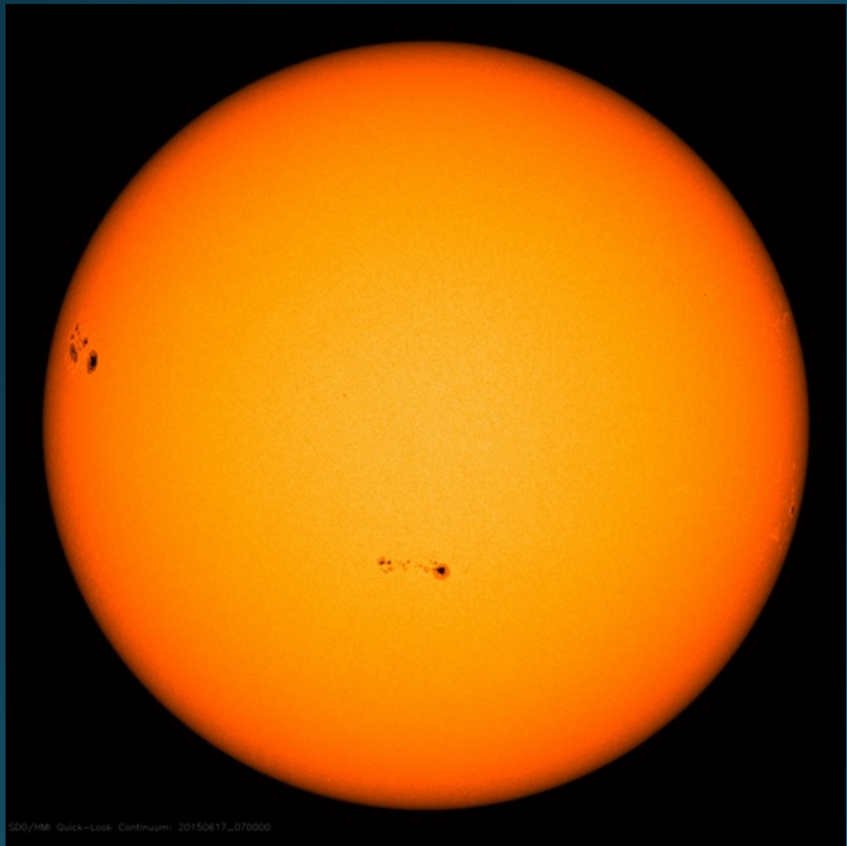

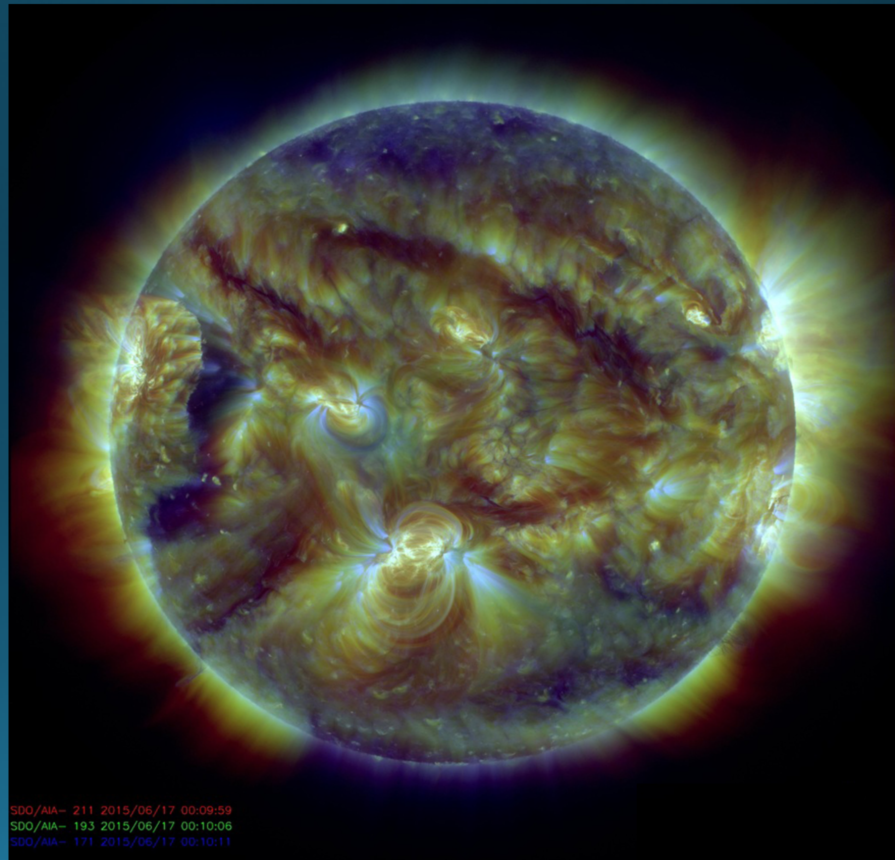

Residuals of solar activity modelling

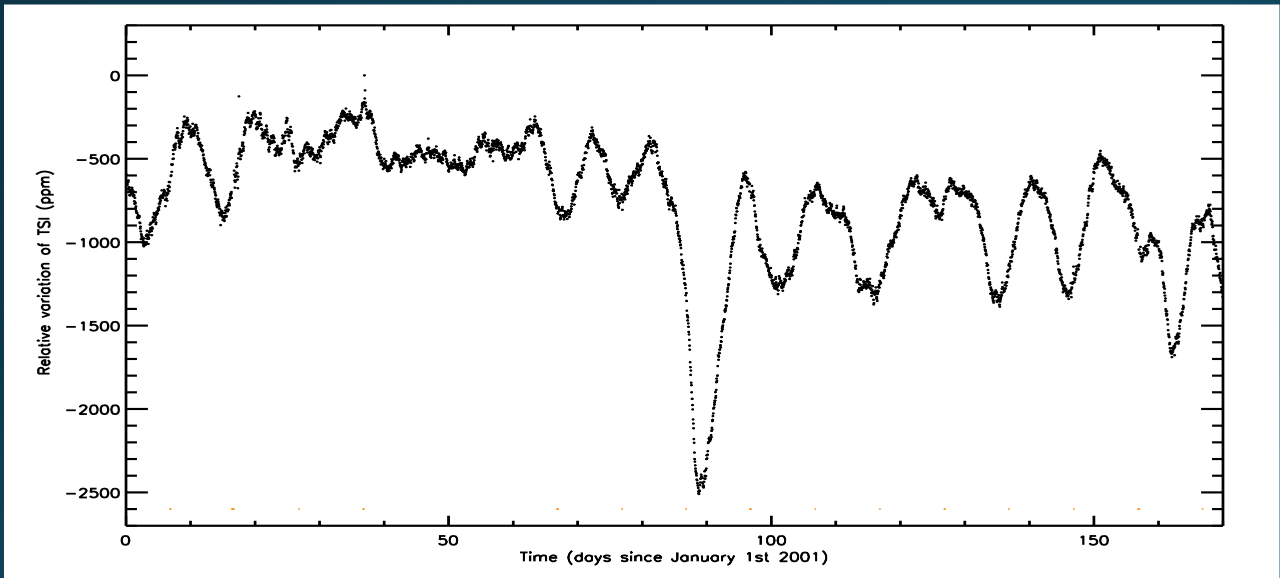

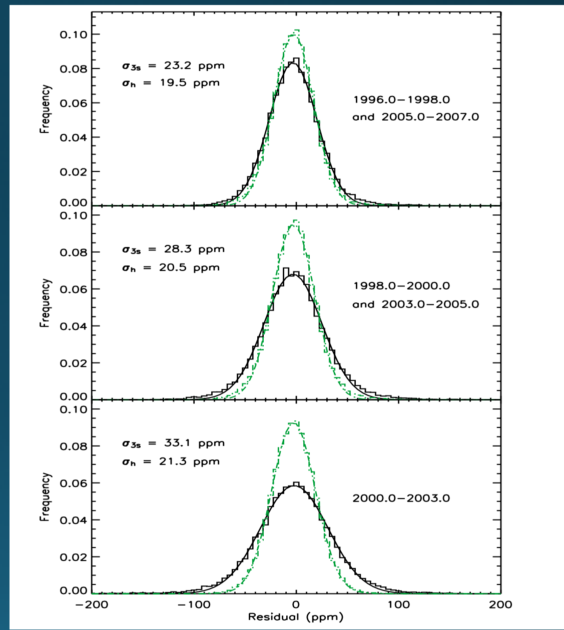

In the case of the Sun (P_{rot} = 25 days) the amplitude of the light curve is of about 0.3%. Application of spot modelling gives residuals with standard deviation of 20-30 ppm.

An active star: Kepler-17

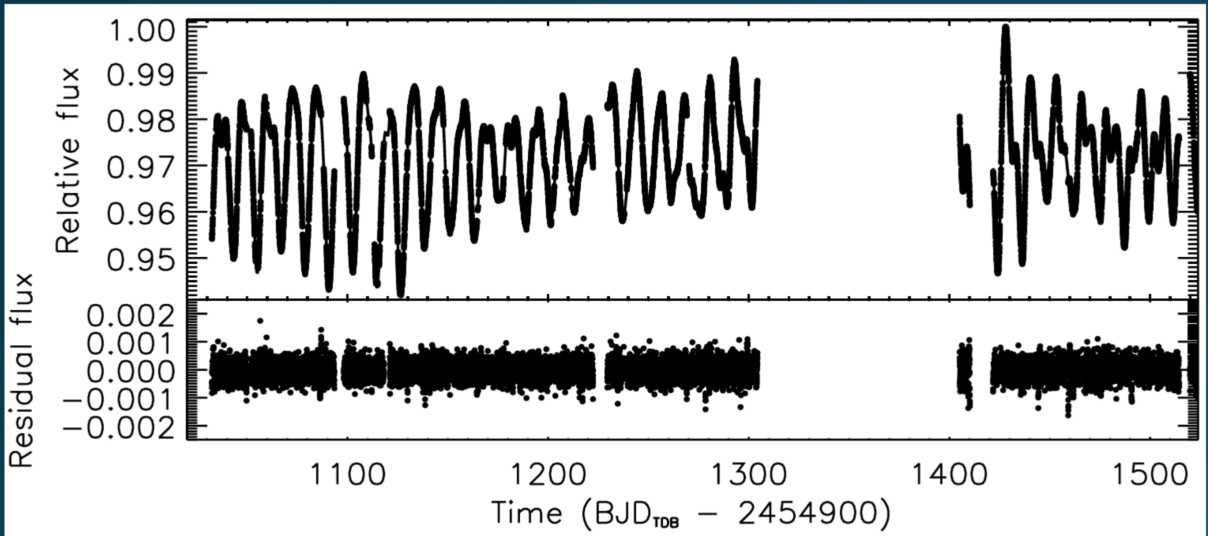

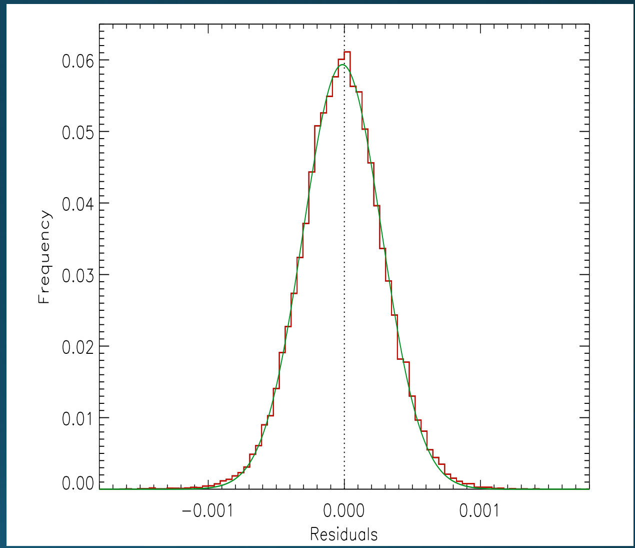

Kepler-17 is a G2V star with a rotation period of 12 days and an estimated age younger than 1.8 Gyr. The amplitude of its light curve is of about 6%, but the standard deviation of its residuals after spot modelling is only 269 ppm, close to the precision of the photometric measurements of 222 ppm.

Solar TSI power spectrum

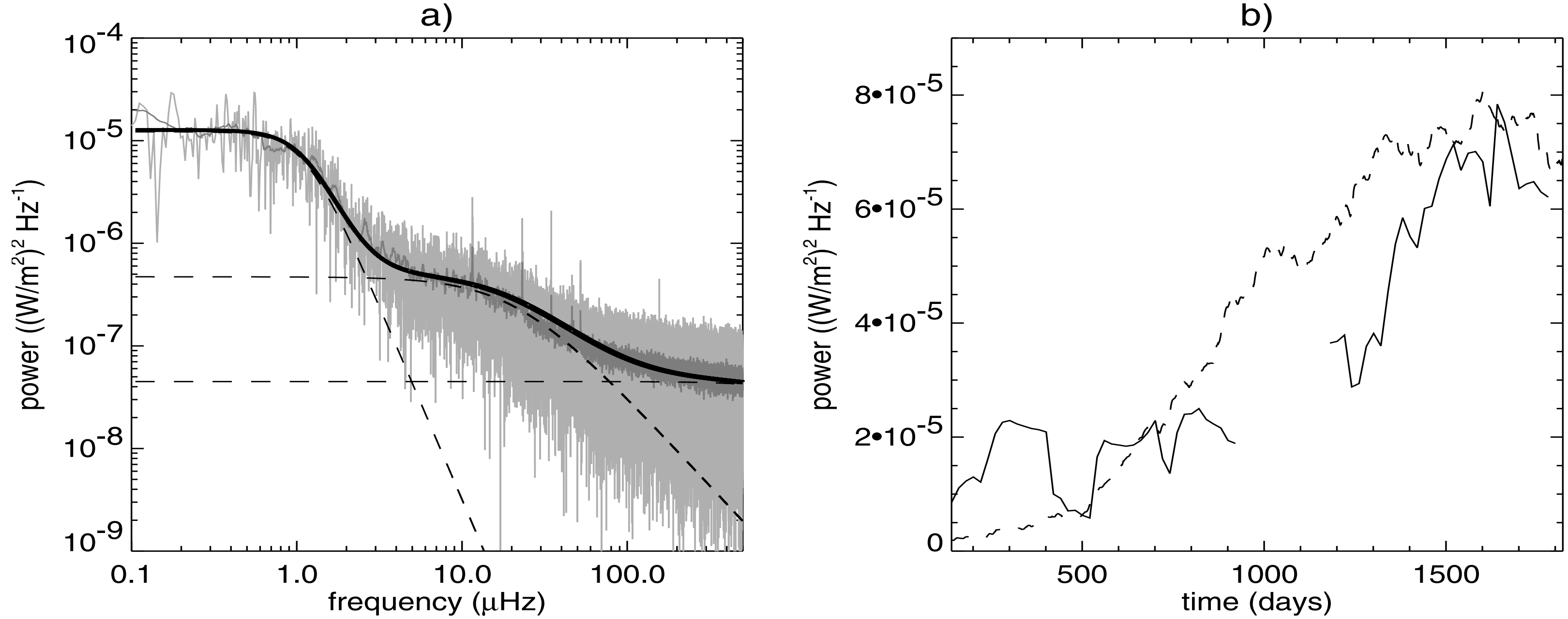

Fig. 2. a) Power spectrum of the PMO6 light curve (1996-2001). Light grey: power spectrum. Dark grey: idem, smoothed with a boxcar algorithm. Thick solid line: multi-component powerlaw fit (see Sect. 2.2). Dotted lines: individual components of the fit. **b)** Comparison between the the time dependence of the amplitude of the low frequency component of the power spectrum (A_1) and chromospheric activity. Solid line: evolution of A_1, computed as described in Sect. 2.3, using L = 180 days and S = 20 days, between 1996 and 2001. The gap at around 1000 days corresponds to a prolonged gap in the data. Dotted line: BBSO Ca II K-line index over the same period (arbitrary units), smoothed with a boxcar algorithm (base 180 days).

Aigrain et al. (2004)

HD173701 vs. the Sun (detail)

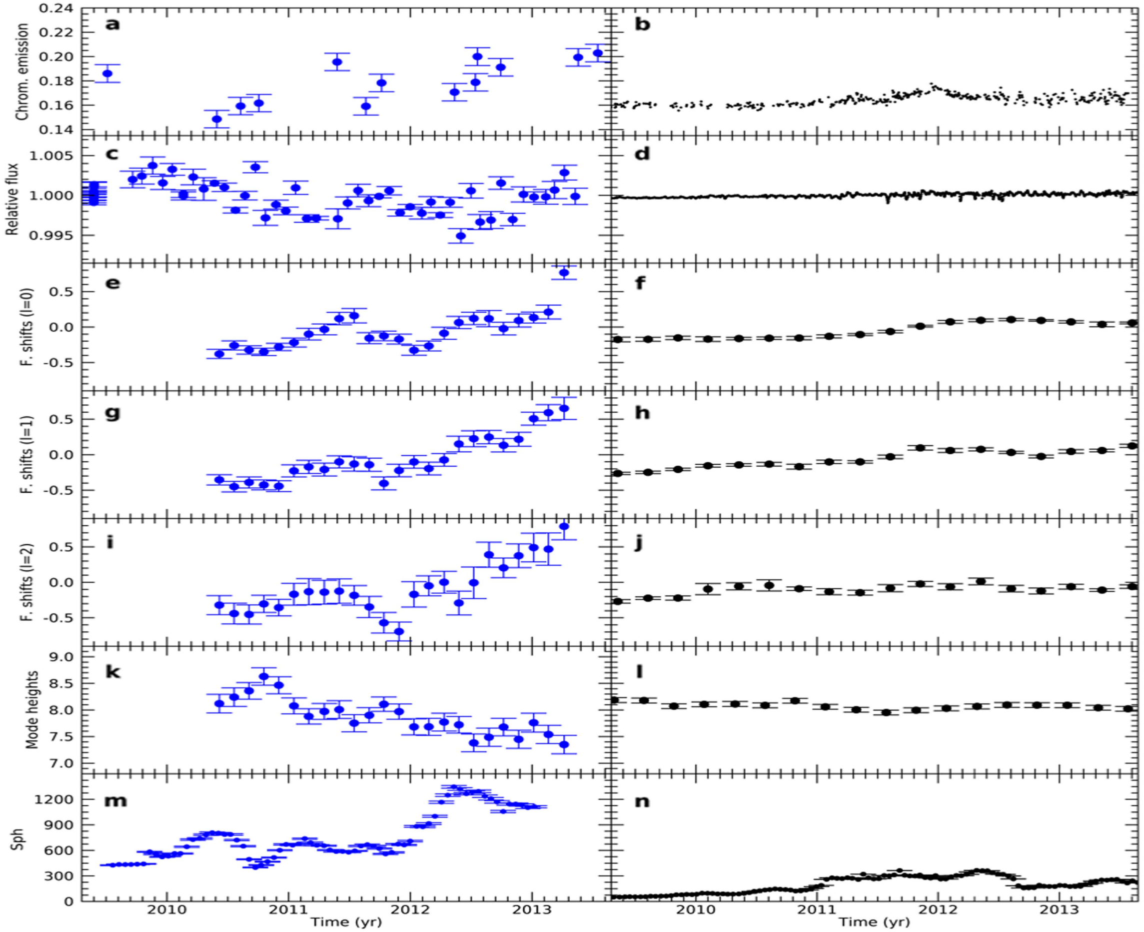

Figure 4. Rising phase of the last cycle in HD 173701 compared to the Sun. The panels show the chromospheric emission (panels (a) and (b)), the relative flux (panels (c) and (d)), radial frequency shifts (panels (e) and (f)), dipolar frequency shifts (panels (g) and (h)), quadrupolar frequency shifts (panels (i) and (j)), logarithmic mode heights of the eigenfrequencies (panels (k) and (l)), and photospheric activity proxy (panels (m) and (n)).

(Karoff et al. 2018)